

# Studying morphosis with a simulated model of the long-tailed lizard *Takydromus sexlineatus*: tail amputation

Konstantinos Karakasiliotis

**Abstract**—Morphology is an important factor in locomotion. It may guide the control strategies that an animal or a robot uses for efficient locomotion. Based on our previous work for the modeling of the long-tailed lizard, in this paper we explore the effect of tail loss, a morphological feature that is particularly distinctive in this species. The main aim is to postulate and possibly predict the changes in the locomotor strategies and performance of an amputated long-tailed lizard. For our study we use optimization algorithms and we mainly focus on the results from the standard PSO (particle swarm optimization). Overall the effect of tail loss does not alter much the behavior of the model, both in terms of postural kinematics and speed performance. However some results show particular interest: first the amputated model uses half the power for achieving the same performance as the intact one, second the amputated model uses wider foot placement for the hind limbs and significantly smaller spinal oscillatory amplitudes. These results may predict that an amputated animal will experience stability problems at higher frequencies.

## I. INTRODUCTION

When it comes to fast, stable and adaptive locomotion, lizards are one of the best animal groups to study. Moreover, lizards display a wide range of morphological diversity and ecological adaptations, including the ability to locomote on a variety of substrates [1]. Lizard locomotor mechanics are remarkably similar to those of other legged animals [2] which suggests that similar locomotor strategies might be shared with other tetrapod groups. Understanding how specific morphological variations affect the locomotion strategies of animals may reveal the principles that connect morphology and control. Moreover, understanding the principles that connect morphology and control is particularly useful for robotics; it can guide the design of a robot for a particular task and provide a good basis for efficient and stable control.

Within the lizard taxon (Lacertilia), in the family of Lacertidae all members are relatively closely related. This increases the chances that observed morphological diversity within this family reflects functional diversity, and not phylogenetic diversity.

Within the Lacertidae, two species, the *Lacerta vivipara* and *Takydromus sexlineatus* have similar body size and they display a general “lizard” body shape, i.e. with not extremely strong (as is specialist runners) or underdeveloped (as in scincids) limbs. The specialist, *T. sexlineatus*, differs from the generalist *L. vivipara* mainly in one, clear, distinguishing feature: extreme tail elongation ([3]–[5]). This should facilitate interpretation of biomechanical comparisons between



Fig. 1. Snapshot of the long-tailed lizard during the experiments.

these species. *Lacerta* is the generalist reference, and a considerable amount of literature is available on general characteristics of lizard locomotion ([2], [6], [7]). Therefore, the main focus of our study is on *Takydromus* (Fig. 1) because it sports a clear case (tail elongation) of long-term morphosis. In the future, similar studies with *L. vivipara* could suggest potential differences in the locomotion control between these two species.

In our previous study [8] we developed a simulated model of the long-tailed lizard able to replicate the speed-frequency response of the real animal. Our exploration was based on systematic tests for 10 control parameters on an intact model (i.e., with the same morphology and inertial characteristics of an intact animal). In this paper our goal is two-fold: i) first to deeper explore the performance of the intact lizard model using Particle Swarm Optimization and Viability Evolution. Optimization in a continuous space can provide better insight for the maximal performance of the model compared to the low resolution quantized systematic tests. ii) second to explore the effect of tail loss (intraspecific morphosis) on the locomotion control of the long-tailed lizard model.

## II. THE LONG-TAILED LIZARD MODEL

### A. Morphology and joints’ topology

In [8] we developed a model of the long-tailed lizard in the ODE-based simulation platform Webots<sup>TM</sup>. The segmentation, geometry and inertial properties of the model are based on the lizard’s morphometric measurements. The spine of the lizard model is composed of 16 active degrees of freedom (DoF) with vertical axis of rotation and 5 passive compliant DoF of which 4 enable vertical movements and the last one rolling movements along the body-axis (Fig. 2). Each limb is composed of 3 active DoF and implemented as a pitch-yaw-knee manipulator. The pitch moves the limb vertically (adduction-abduction), the yaw, horizontally, back and forth (retraction-protraction) and the knee extends and retracts the foreleg.

For this study, additionally to the previous model, we used an amputated model. The tail was removed at a position close to the body (Amputation plane in Fig. 2). The tail should

not be removed from its connection to the trunk as in real animals some part of the tail is always needed for anatomical reasons (animal’s vent).

### B. Control

We use position control for all active DoF of the model with relatively high PID gains. This ensures that the defined postures and trajectories are respected, even in high frequencies.

1) *Spine*: The spine is controlled by a simple sine controller. The angle of each active DoF,  $\theta_i$ , is given by:

$$\begin{aligned} \theta_i &= A_i \sin(\phi + \psi_i), \quad 1 \leq i \leq 16 \\ \phi &= 2\pi ft \end{aligned} \quad (1)$$

where  $\phi$  is the phase of the locomotion cycle,  $f$  its frequency,  $t$  the time,  $A_i$  the amplitude of the  $i$ -th joint and  $\psi_i$  the phase difference between the phase of the  $i$ -th joint and the phase of the locomotion cycle.

2) *limbs*: We control the limbs in the end-effector trajectory space, i.e., we define a trajectory for each foot which is followed precisely throughout the cycle. The reference frame for each pair of limbs (front and hind) is defined as the midpoint between shoulders or hips (Fig. 2). The  $x$ -axis of the reference frame is always parallel to the line of locomotion. The  $y$ -axis is on the vertical direction and the  $z$ -axis on the lateral. A trajectory is defined by a set of three trigonometric equations, one for each axis. A point  $\mathbf{p} = (x, y, z)$  of this trajectory is given by:

$$\begin{aligned} x &= A_x \sin(\phi + \xi) + X \\ y &= \begin{cases} A_y \cos(\phi + \xi) + Y & \text{if } \cos(\phi + \xi) \leq 0 \\ Y & \text{else} \end{cases} \\ z &= \begin{cases} A_z \cos(\phi + \xi) + Z & \text{if } \cos(\phi + \xi) \leq 0 \\ Z & \text{else} \end{cases} \end{aligned} \quad (2)$$

where  $A_{x,y,z}$  represent the amplitude of the movement at each axis and  $X, Y, Z$  the corresponding offsets.  $\phi$  is, as before, the phase of the locomotion cycle and  $\xi$  the phase lag between the phase of the foot and  $\phi$ . In other words, the foot follows a kind of semicircular trajectory. In stance phase, it follows a straight trajectory (of length  $2A_x$ ), backwards, at constant offsets  $Y$  and  $Z$  from the reference frame of the limb. The offset  $X$  defines the front-back asymmetry of the stride around the shoulder/hip, i.e. positive  $X$  would retract the foot more than protract it. In swing phase the foot is cleared from the ground up to a height  $A_y$  and extended from the body at a distance up to  $Z + A_z$ . Thus, the above 6 variables are the ones to control the shape of a trajectory. The calculation of the inverse kinematics for the limb joints are presented in [8]. The control variables will be further discussed in the optimization section.

## III. OPTIMIZATION

### A. Optimization algorithms

We made extensive use of the standard PSO (particle swarm optimization) and we tested a new evolutionary algorithm, the Viability Evolution described in [9]. The particle swarm optimization is a very elegant, simple and

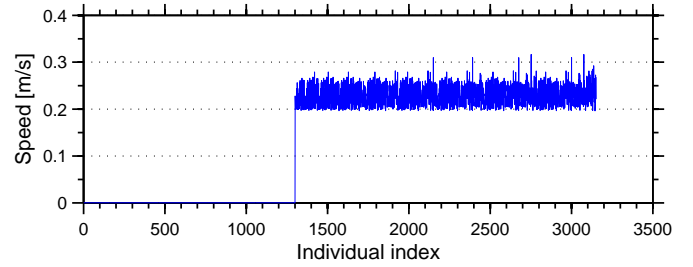


Fig. 3. Example of the ViE performance. The plot shows the evolved speed. The expected speed was around 0.6m/s while the algorithm found much slower solutions (at the given number of individuals).

fairly recent optimization algorithm [10], [11]. It is loosely based on the notion of swarm/flocking behavior. On the other hand, Viability Evolution (ViE) is an evolutionary algorithm based on iteratively reshaping constraints which define the viable space of solutions. The reproduction of individuals is not based on explicit fitness but rather on elimination according to the “environmental” constraints. ViE has proved to preserve diversity and therefore explore more solutions, however, in terms of implementation, contrary to PSO, it cannot be parallelized, demanding more (real) time for it to converge.

In our preliminary analysis<sup>1</sup> we found that ViE may not be very well suited for the lizard’s optimization landscape. The landscape can be “flat” for several individuals and iterations mainly because of the small ranges in which the inverse kinematics of the limbs can find a valid solution (see Design of Experiments for details on the optimized parameters). This probably caused the ViE algorithm to be either very slow (in terms of convergence) or to oscillate around a suboptimal solution (compared to the expected one from the systematic tests). An example of the ViE output is shown in Fig. 3. In the figure, the speed of all individual is much slower than the expected one (see Results section).

### B. Design of experiments

The simulated long-tailed lizard has a total of 64 control parameters. In our previous study we reduced this number to 11 based on several hypotheses. We used the same parameters both for the intact lizard model and the amputated one. Those parameters are: 1) the amplitude of body oscillation,  $A$ , 2) the frequency,  $f$ , 3,4) the protraction-retraction range of the forelimbs and hind limbs,  $A_x$ , 5) the distance of the shoulders from the ground,  $Y^{FL}$ , 6) the distance of the hips from the ground,  $Y^{HL}$ , 7,8) the lateral placement of the front and back feet from the line of locomotion,  $Z^{FL}$  and  $Z^{HL}$  respectively, 9,10) the offset of the protraction-retraction oscillation with respect to the hips and shoulders,  $X_{HL}$  and  $X_{FL}$  and 11) the duty factor  $D_f$  (ratio of stance duration over the locomotor cycle duration). The selected ranges for each variable are shown in Table I. Note that the frequency was not used as an open parameter for the

<sup>1</sup>We were able to run only a single experiment using ViE and therefore not explored several possible configurations of the algorithm.

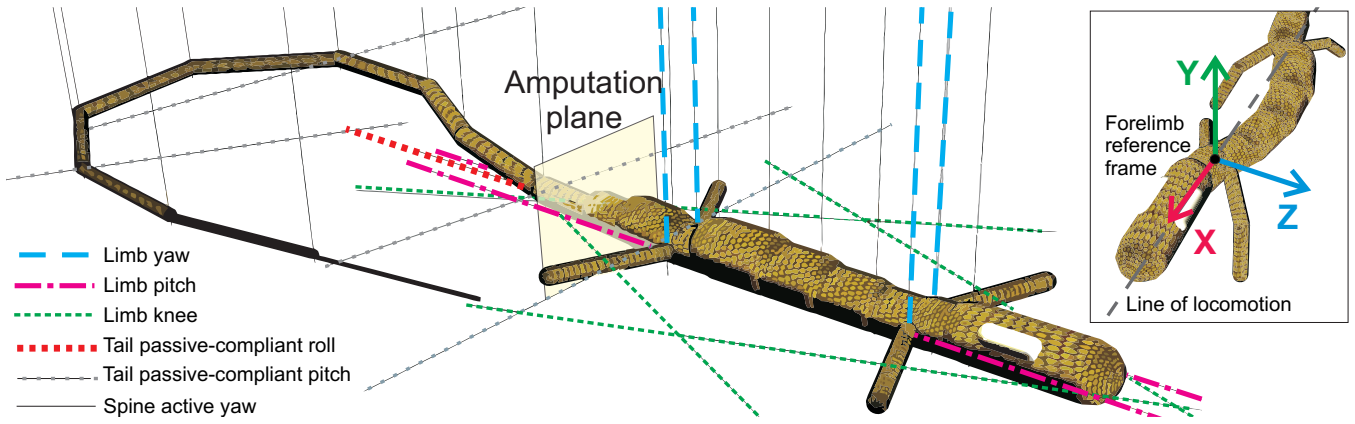


Fig. 2. The long-tailed lizard model. Definitions of the active and passive DoF denoted with different line styles and colors. (top right) Illustration of the line of locomotion and the reference frame of the forelimbs (the definition is similar for the hind limbs).

TABLE I  
OPTIMIZATION PARAMETERS AND BOUNDARIES

Variable	Low	High	Unit
$A$	0	0.3	rad
$f$	4	9	Hz
$D_f$	20	80	%
$A_x^{HL}$	5	15	mm
$X^{HL}$	-5	5	mm
$Y^{HL}$	-5	5	mm
$Z^{HL}$	-5	5	mm
$A_x^{FL}$	5	15	mm
$X^{FL}$	-5	5	mm
$Y^{FL}$	-5	5	mm
$Z^{FL}$	-5	5	mm

## IV. RESULTS

### A. Frequency response of metrics

In our previous work [8] we showed that the frequency response of the model, explored through systematic tests, was surprisingly close to the real data. For convenience those data are shown also here in Fig. 4. The black line with diamonds shows the results from the systematic tests and the real animal data are shown with green circles.

Interestingly, the optimization process, for the intact lizard model (blue squares), found a much faster solution for all the frequency levels. This suggests that relatively small changes in the coordination of the different DoF of the model may alter significantly its speed. The difference between the real data and the optimal speed achieved by the model may also suggest that the speed is not the only metric that animals account for (energy efficiency could be a second). Moreover, the mean optimal speeds of the amputated lizard model (red triangles) are almost identical, in most cases, with the intact's. The latter might not be very surprising as the main propulsion comes from the limbs and the bending of the trunk while the optimization process does not take into account the energy needed to achieve the same goal. Indeed, a plot of the effort of the two models for their optimal speed per frequency level shows that the amputated model is twice as efficient (Fig. 5).

The above results show that a more sophisticated fitness function, e.g. efficiency, could give results closer to the ones recorded from the animal in future experiments. A second observation that would demand further exploration is the effort-frequency response of the intact lizard model (blue squares; Fig. 5). Contrary to the effort response of the amputated model, which is linear, the intact model seems to use approximately the same effort for frequencies higher than 6 Hz, although its speed increases (blue squares; Fig. 4). This might mean that the model exploits the passive components of its joints, e.g. all the passive DoF in the tail (which are not present in the amputated model), and the compliant ground contact model.

The evolution of the best individuals for each iteration of

individual optimization runs, but several optimizations were performed for different levels of frequency, every 1 Hz. In particular at least 5 optimization runs were performed for each frequency level. Whenever the results of similar optimization runs were not close to each other, up to 10 runs were performed in order to enhance the reliability of our conclusions.

For the fitness we measured only the speed of forward locomotion. However, a measure of the power consumption was recorded parallel to the fitness which we call effort. Effort is calculated as the sum of the squares of the joint/motor torques. The latter, although does not precisely give the power consumption (this would mean that a precise model of the motors is available), it gives a fairly good approximation of it.

In total, 68 different PSO optimizations were performed. Initial exploration for the number of iterations needed showed that 150 iterations for the intact model and 200 iteration for the amputated model were enough to ensure convergence. In both cases the number of particles was 50. This means that 7500 and 10000 individuals respectively were explored in each optimization run.

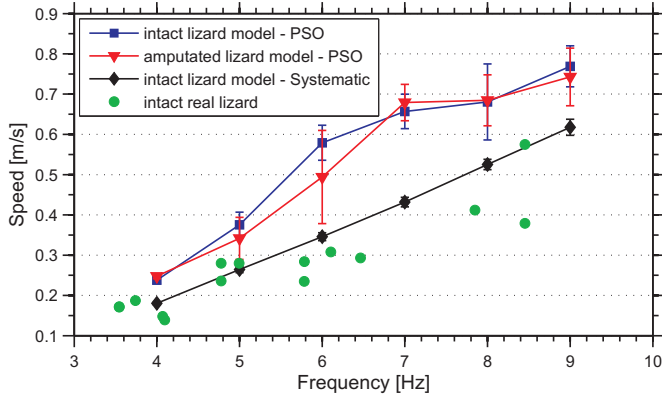


Fig. 4. Speed-frequency responses of the intact model using PSO (blue squares), the amputated model using PSO (red triangles), the intact model using systematic tests (black diamonds; data from [8]) and real animals (green circles; data from [8]).

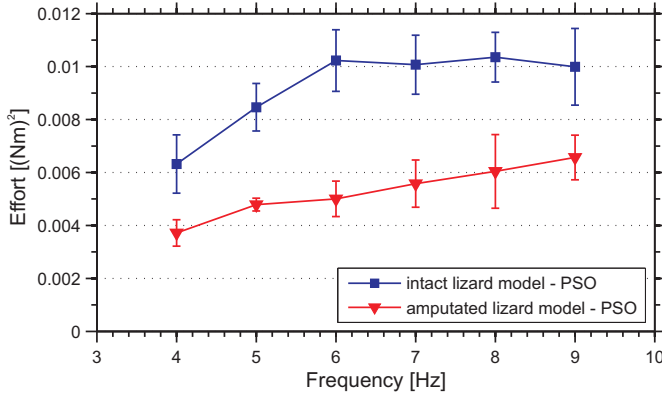


Fig. 5. Effort-frequency responses of the fastest intact model using PSO (blue squares) and the fastest amputated model using PSO (red triangles).

the different optimizations for the intact and the amputated model is shown in Fig. 6 and 7 respectively. Two observations can be made from the two figures: i) The majority of the optimization runs converged to a similar solution and ii) the majority of the optimizations converged to a solution close to their best in less than 50 iterations. The two observations show that the PSO works robustly and fast for the current problem.

### B. Analysis of optimized control parameters

That the speed seems to have converged after the 50<sup>th</sup> iteration for most of the optimization runs, it should not necessarily mean that the combination of the 10 control parameters is the same. A deeper analysis in the evolution of each parameter along the iterations of different optimizations showed that in our case similar values are used among best individuals (i.e. all the parameters followed a straight line after almost the 50<sup>th</sup> iteration; Fig. 8 and 9). Some variability may also appear between different optimization runs of same parameters, i.e. different optimization runs may converge to the same speed but with different control parameters. Very few cases however show such a significant variability in our

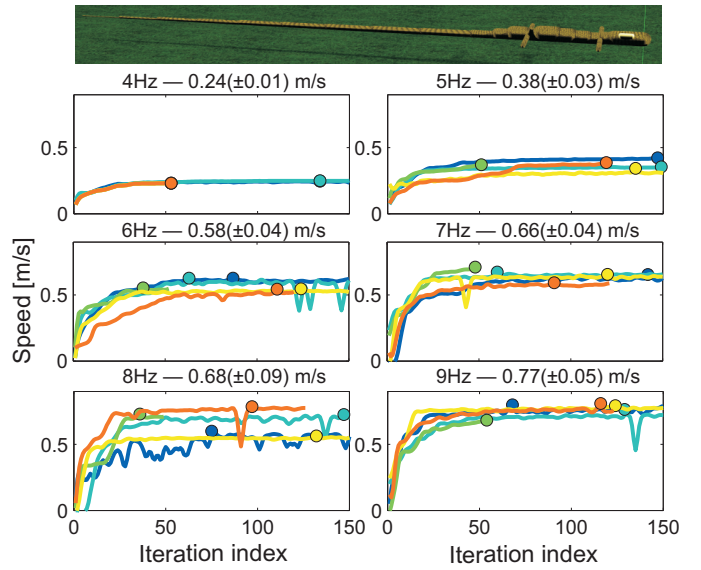


Fig. 6. Optimization process of the intact long-tailed lizard model. Evolution of the best individual for all the iterations of different optimization runs (different colored curves) for the different levels of frequencies (different plots). The colored circles denote the best individual for each run. The title of each plot gives the mean and standard deviation of the best individuals.

experiments with the majority of the parameters converging at similar values.

The optimized control parameters of the intact and the amputated models are more clearly shown in Fig. 10. For each frequency level, the parameters of the best individual of each optimization were selected for the calculation of the mean and standard deviation of each single parameter. The blue circles correspond to the values used by the intact model while the red triangles by the amputated.

From our previous systematic tests [8] we suggested that the optimal posture for a model with the morphology of the intact long-tailed lizard is the following: i) The hips should be kept close to the ground and the hind feet far from the body-axis (laterally) and ii) The shoulders should be higher than the hips and the front feet close to the body-axis. The results from the optimization of the intact model show the same pattern (Fig. 10; blue lines and circles). In particular, the hip height (Fig. 10E) is always slightly lower than the one of the shoulders (Fig. 10F). Also, the hind feet (Fig. 10G) are placed in a wider posture than the front ones (Fig. 10H) for the majority of the cases.

In terms of control, the intact model (blue circles in Fig. 10) shows a quite variable behavior for the spinal oscillatory amplitude (Fig. 10I) with the lowest bending found at the two extremes of the frequency range and the highest inbetween. The duty factor (Fig. 10J), more obviously in low frequencies, shows a slight tension to decrease which means that the model goes from walking to running gaits as frequency increases. Although the retraction range (how much they move back and forth) of the hind limbs is not significantly variable, the forelimbs seem to slightly decrease their range as the frequency increases. The latter could mean

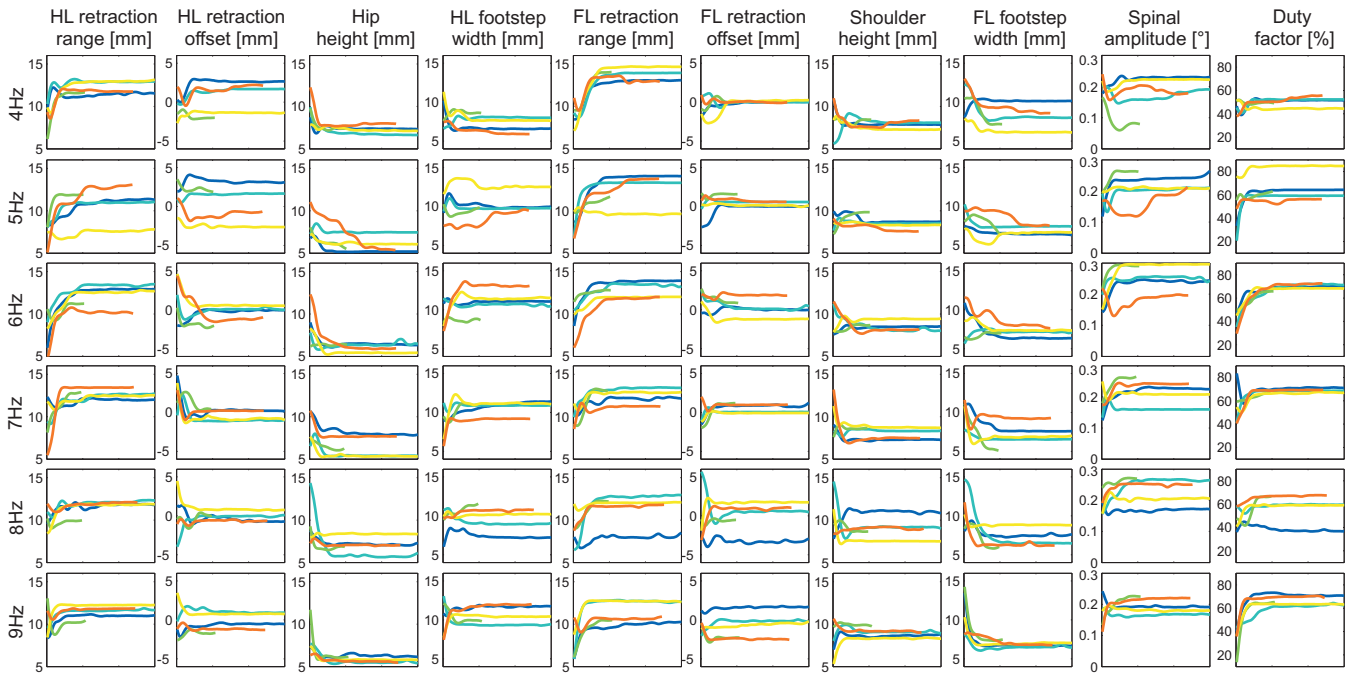


Fig. 8. Evolution of each control parameter of the intact long-tailed lizard model with respect to the iteration number for all optimization runs.

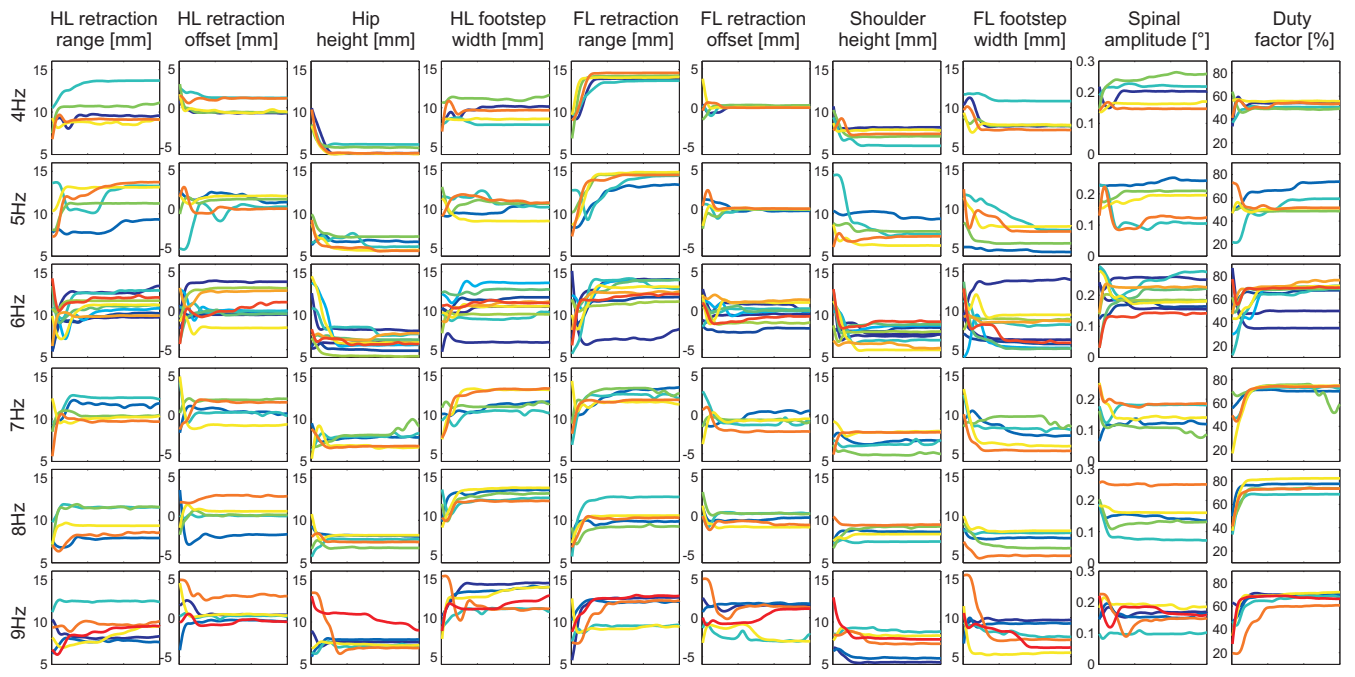


Fig. 9. Evolution of each control parameter of the amputated long-tailed lizard model with respect to the iteration number for all optimization runs.

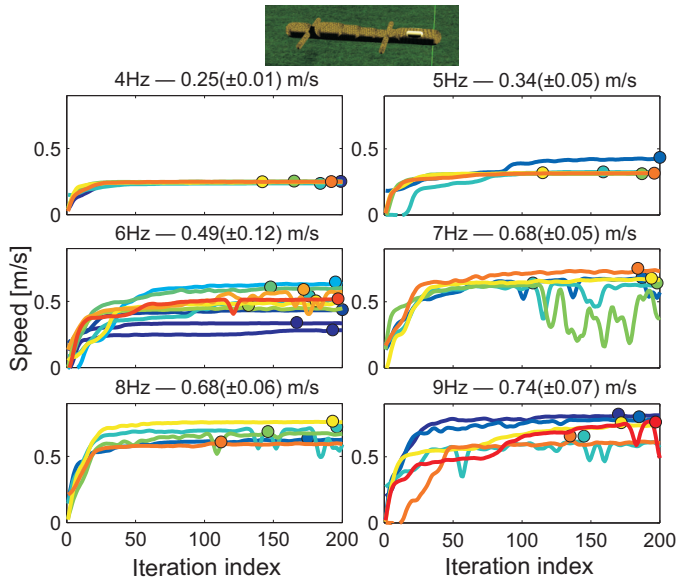


Fig. 7. Optimization process of the amputated long-tailed lizard model. Evolution of the best individual for all the iterations of different optimization runs (different colored curves) for the different levels of frequencies (different plots). The colored circles denote the best individual for each run. The title of each plot gives the mean and standard deviation of the best individuals. Note that for some frequencies (e.g. 6 Hz) more runs were needed because of the spread of the converged results.

that the role of the forelimbs slightly decays as the frequency and thus speed increases. That the retraction offset of both the hind and forelimbs remains close to zero, it means that the model prefers to use symmetric protraction and retraction around the hips and shoulders.

Overall, the effect of tail loss did not seem to alter much the behavior of the long-tailed lizard model (red triangles; Fig. 10). The trend of each variable with respect to the frequency remained the same or very similar. Only a few parameters were affected. The amplitude of spine undulations was significantly reduced for frequencies higher than 4 Hz (Fig. 10I). The lateral placement of the hind feet was also increased for most of the frequencies (Fig. 10G) while the front feet showed the same exact values as for the intact model (Fig. 10H). The two latter observations may suggest that the tail loss reduces stability as smaller amplitudes and wider hind feet placement yield more stable gaits. Another small change appears at the relative heights of the hips and shoulders. The amputated model uses slightly more balanced (parallel to the ground) posture for the trunk (Fig. 10E and F). This might be related to the reduced weight at the model's hips due to the tail loss. Finally, the retraction range of the hind limbs is reduced in the amputated model (Fig. 10A) probably because the propulsion from the front feet is enough to pull the model forward. The additional friction induced by the contact of the tail with the ground and due to the higher normal forces at the hind limbs may increase the importance of the hind limbs' retraction range.

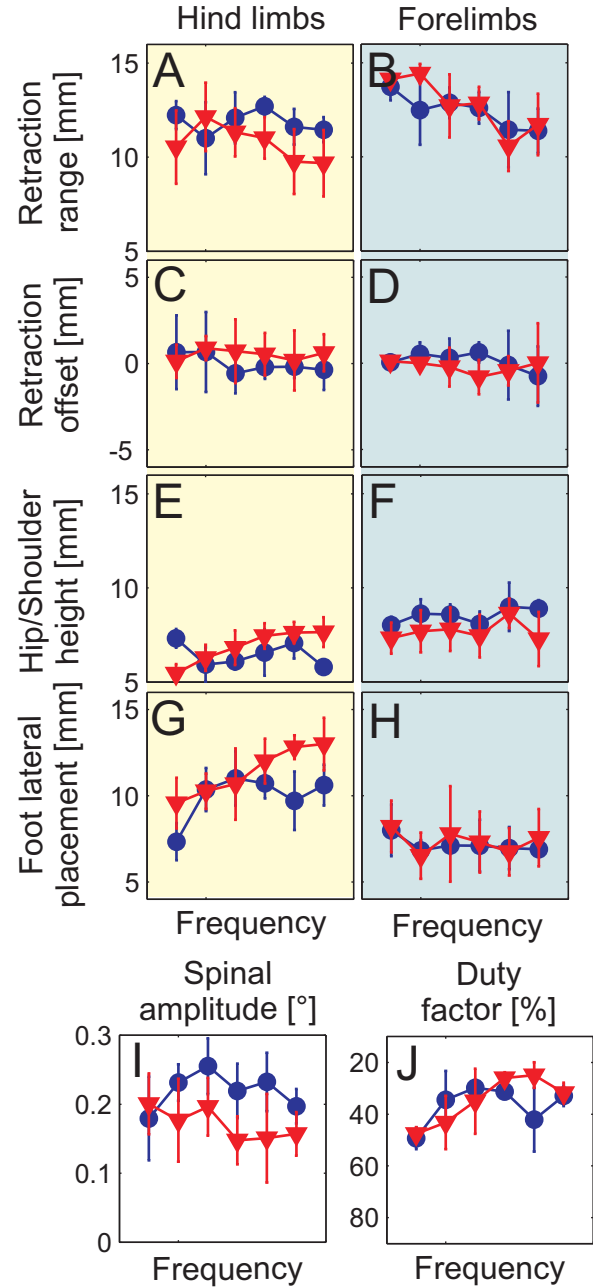


Fig. 10. Analysis of the optimized parameters. Each plot shows the mean and standard deviation (error bars) of a single optimized parameter of the intact long-tailed lizard model (blue squares) and the amputated model (red triangles) as a function of the different frequency levels (4 – 9 Hz). The mean values are calculated from several optimization levels runs of the same frequency. (A, B) Protraction-retraction range of the hind limbs and forelimbs,  $A_x^{HL}$  and  $A_x^{FL}$ , (C, D) Offset of the protraction-retraction oscillation with respect to the hips and shoulders,  $X_{HL}$  and  $X_{FL}$ , (E, F) Height of the hips/shoulders from the ground,  $Y^{HL}/Y^{FL}$ , (G, H) Lateral placement of the hind and front feet from the line of locomotion,  $Z^{HL}$  and  $Z^{FL}$  respectively, (I) Amplitude of body oscillation,  $A$ , (J) Duty factor  $D_f$ .

## V. CONCLUSIONS AND FUTURE WORKS

The analysis of the long-tailed lizard's locomotion through optimization has confirmed our observations related to the animal's posture from previous systematic tests. However, the optimization using speed as a fitness failed to reproduce the animal data. Our hypothesis is that animals account for efficiency and therefore more sophisticated fitness functions should be explored in the future. In terms of morphosis, we explored the effect of tail loss by comparing the intact with the amputated model over the same set of parameters. That the overall behavior of the model did not change significantly it should not be unexpected as the tail does not, potentially, play a big role in ground propulsion. However, two interesting hypotheses and possibly predictions can be made for the walking behavior of an amputated long-tailed lizard: 1) the animal could be more unstable and to compensate for this it would use a wider posture for the hind feet and reduced body undulations. 2) it would use more level trunk postures (parallel to the ground) and the hind limbs would reduce their protraction-retraction range.

In the future it would be interesting to look into data from real amputated animals and evaluate our predictions. Moreover, apart from the more sophisticated fitness functions, other types of environments should be explored, e.g. sloped terrain and different ground friction coefficients.

## VI. ACKNOWLEDGMENTS

The research leading to these results has received funding from the European Community's Seventh Framework Programme FP7/2007-2013 - Future Emerging Technologies, Embodied Intelligence, under grant agreement no. 231688. The author acknowledges also the help of Andrea Maesani for his help for setting up the AEON framework.

## REFERENCES

- [1] Aerts, P. and Van Damme, R. and Vanhooydonck, B. and Zaaf, A. and Herrel, A. (2000). Lizard Locomotion: How Morphology Meets Ecology. *Netherlands Journal of Zoology* 261, 0028-2960.
- [2] Farley, C. T. and Ko, T. C. (1997). Mechanics of locomotion in lizards. *Journal of Experimental Biology* 200, 2177-2188.
- [3] Martin, J. and Avery, R. A. (1998). Effects of tail loss on the movement patterns of the lizard, *Psammmodromus algirus*. *Functional Ecology* 12, 794-802.
- [4] Brown, R. M., Taylor, D. H. and Gist, D. H. (1995). Effect of caudal autotomy on locomotor performance of Wall Lizards (*Podarcis muralis*). *Journal of Herpetology* 29, 98-105.
- [5] Lin, Z.-H. and Ji, X. (2005). Partial tail loss has no severe effects on energy stores and locomotor performance in a lacertid lizard, *Takydromus septentrionalis*. *Journal of Comparative Physiology B: Biochemical, Systemic, and Environmental Physiology* 175, 567-573.
- [6] Reilly, S. M. and Delancey, M. J. (1997). Sprawling locomotion in the lizard *Sceloporus clarkii*: quantitative kinematics of a walking trot. *J. Exp. Biol.* 200, 753-765.
- [7] Russell, A. P. and V. Bels. (2001). Biomechanics and kinematics of locomotion in lizards: Review, synthesis and prospectus. *Comp. Biochem. Physiol. A* 131:89112
- [8] Karakasiliotis, K., D'Août, K., Aerts, P. and Ijspeert, A. J. (2012) Locomotion studies and modeling of the long-tailed lizard *Takydromus sexlineatus*. Accepted for publication in the proceedings of the Int. Conf. on Biomedical Robotics and Biomechatronics, Roma, Italy.
- [9] Maesani, A., Fernando, P. R. and Floreano D. (2012) Artificial evolution by means of eliminations and environmental changes. Under preparation.
- [10] Kennedy, J. and Eberhart, R. (1995). Particle swarm optimization. *Particle swarm optimization*. ( 4, 1942-1948 vol.4).
- [11] Clerc, M. and Kennedy, J. (2002). The particle swarm - explosion, stability, and convergence in a multidimensional complex space. *Evolutionary Computation*, IEEE Transactions on 6158-73.
- [12] Hildebrand, H. (1966). Analysis of the symmetrical gaits of tetrapods. *Folia Biotheoretica* 4, 922.
- [13] Kostas Karakasiliotis and A.J. Ijspeert (2009), "Analysis of the terrestrial locomotion of a salamander robot", In *Proceeding of IEEE IROS09*, St. Louis, USA.